Available Online: 25 August 2026 DOI: 10.54254/3029-0821/2026.36335

Engineering Escherichia coli for targeted biosynthesis of neohesperidin as an adjuvant therapeutic strategy for colorectal cancer

Annabella Dai

Orange County School of the Arts, Los Angeles, USA

bellashdai@gmail.com

Abstract. Colorectal Cancer (CRC) is the third most prevalent cancer and the second most deadly cancer in the world, and current treatments have significant side effects and drug resistance. Citrus plants contain flavonoids glycosides, such as neohesperidin, which has antioxidant, anti-inflammatory, immunomodulatory and antitumor properties, making it a promising CRC adjuvant. However, conventional extraction is limited by low natural abundance, poor consistency and low bioavailability. In this study, E. coli BL21 (DE3) were engineered to produce neohesperidin de novo from naringenin by two integrated modules that convert naringenin to hesperetin and then to neohesperidin. The neohesperidin yield reached 4.55 mg/L using naringenin as the substrate. These findings provide a precision, scalable platform for adjuvant CRC therapy.

Keywords: neohesperidin, microbial biosynthesis, metabolic engineering, colorectal cancer

1. Introduction

1.1. Global burden of colorectal cancer

Colorectal Cancer (CRC) is the third most commonly diagnosed cancer worldwide and was the second leading cause of cancer death in 2020 [1, 2]. The global CRC burden is projected to more than double by 2035, with the steepest increases in low- and middle-income countries with limited screening infrastructure. Of particular concern, CRC is increasingly diagnosed at younger ages, and its incidence is rising among people younger than 50 years [3]. CRC usually develops through the adenoma-carcinoma sequence over approximately 10-15 years, a process driven in part by chronic intestinal inflammation. Such inflammation can disrupt immune surveillance, impair epithelial barrier function and activate oncogenic pathways, including NF-κB and Wnt/β-catenin signalling.

1.2. Limitations of current treatments

Current treatments for CRC include surgery, chemotherapy, radiotherapy, targeted therapy and immunotherapy. Although these approaches can improve survival, each has substantial limitations. FOLFOX- and FOLFIRI-based chemotherapy causes toxicities, including myelosuppression, neuropathy and nausea, in

up to 60% of patients. Molecularly targeted agents are costly and often engender acquired resistance during treatment. Moreover, only a small subset of patients with Microsatellite Instability-High (MSI-H) or Mismatch Repair-Deficient (dMMR) tumours respond to PD-1 blockade. More effective, safer and more accessible treatments are therefore urgently needed [4].

1.3. Neohesperidin as a candidate adjuvant therapy

Neohesperidin is a naturally occurring flavanone glycoside found mainly in the peels of citrus species, including Citrus aurantium and Citrus reticulata. It is also an important bioactive constituent of several traditional Chinese medicines. Neohesperidin exhibits antioxidant activity through free-radical scavenging [5] and anti-inflammatory activity through inhibition of NF-κB/p65 and MAPK signalling. It also has immunomodulatory and antitumour activities mediated through multiple mechanisms [6].

Additional pharmacological activities have also been reported, including antidiabetic effects in vitro [7] and neuroprotective effects in vivo, where oral neohesperidin attenuated MPTP-induced neurodegeneration by modulating inflammatory responses and the gut microbiota [8, 9].

In CRC, neohesperidin suppresses colitis-associated colorectal tumour development, reshapes pro-tumour gut microbial communities and arrests cancer-cell cycle progression. It also enhances the cytotoxicity of 5-Fluorouracil (5-FU) [10, 11]. Together, these properties support neohesperidin as a candidate adjuvant therapy.

However, production constraints remain a major barrier to the clinical translation of neohesperidin. Its abundance in natural citrus sources is low, reaching only 0.29% in C. aurantium flower buds and 0.0057% in other plant sources. Conventional solvent extraction and multistep chromatographic purification show poor batch consistency, pose residual-solvent risks and typically yield products of no more than 95% purity. The low aqueous solubility and oral bioavailability of neohesperidin further limit its pharmacological activity. Reliable and scalable biosynthetic production strategies are therefore needed to overcome these limitations [12].

1.4. Synthetic biology as a platform for natural-product biosynthesis

Advances in synthetic biology now enable scalable microbial production of complex natural compounds that are difficult to obtain directly from plants. These products include flavonoids, terpenoids, alkaloids and other plant-derived molecules with therapeutic potential.

Escherichia coli is widely used for microbial production because it grows rapidly, has a well-characterized genetic background and supports scalable fermentation. E. coli Nissle 1917 (EcN) is a probiotic strain with decades of clinical use in inflammatory bowel disease and an established safety record in humans [13]. These properties make EcN a promising live biotherapeutic platform for intestinal drug delivery.

1.5. Project rationale and objectives

This project aimed to develop a probiotic E. coli system that can perform three functions: (1) efficient de novo biosynthesis of neohesperidin from readily available flavonoid precursors; (2) activation of the production pathway in response to the tumor microenvironment, which is pH-responsive; and (3) dual-mechanism biosafety control, both in vivo and in the environment, using inducible kill-switch systems. The tumor microenvironment of CRC is highly acidic, with the Warburg effect, which is the tendency of rapidly proliferating tumor cells to primarily use aerobic glycolysis to lower the pH of the microenvironment to around 5.8 to 6.5. This acidity inhibits the activity of cytotoxic immune cells and promotes metastatic activity. This pH difference is an elegant molecular trigger for drug synthesis, which can be used to deliver drugs in a spatially and temporally precise manner without the need for exogenous targeting ligands. The research

reported here is a systematic design, construction and experimental validation of all three functional systems, culminating in a proof-of-concept probiotic platform that combines high efficiency biosynthesis, precision targeting and strong biosafety in a single therapeutic platform for CRC adjuvant therapy.

2. Materials and methods

2.1. Bacterial strains, plasmids and pathway design

Escherichia coli DH5α was used for plasmid construction and propagation, whereas E. coli BL21 (DE3) was used for protein expression and biosynthetic experiments. Biosynthetic constructs were derived from pET28a(+), which contains a kanamycin-resistance marker and an IPTG-inducible T7 promoter. The low-copy plasmid pSB1A3, carrying an ampicillin-resistance marker, was used for inducible reporter and suicide constructs.

The biosynthetic pathway comprised an upstream hesperetin module and a downstream neohesperidin module. In the upstream module, ThF3′H from Tricyrtis hirta and CPR from Arabidopsis thaliana converted naringenin to eriodictyol, which was subsequently methylated by MpOMT from Mentha × piperita to produce hesperetin. In the downstream module, UGT73B2 converted hesperetin to hesperetin 7-O-glucoside. VvRHM-NRS supplied UDP-rhamnose, and Cm1,2RhaT catalysed terminal rhamnosylation through an α- glycosidic bond to produce neohesperidin.

2.2. Plasmid construction and strain verification

Genes were codon-optimized for expression in E. coli and synthesized commercially or amplified from available templates using Phusion or Q5 high-fidelity DNA polymerase. Primers contained approximately 15-bp homologous regions complementary to adjacent fragments or linearized vectors.

The pET28a(+) and pSB1A3 backbones were linearized by PCR and purified by agarose gel extraction. Seamless assembly was performed in a total volume of 10 μL containing 2 μL of assembly premix, 50–100 ng of linearized vector and 50–150 ng of each insert. Reactions were incubated at 50 °C for 15 min. Multigene constructs were generated by sequential assembly or one-step multi-fragment assembly.

Assembly products were introduced into chemically competent DH5α or BL21 (DE3) cells by heat shock at 42 °C for 90 s. After recovery in 500 μL of LB medium at 37 °C and 200 rpm for 1 h, cells were plated on LB agar containing kanamycin (50 μg/mL) or ampicillin (100 μg/mL). Positive colonies were screened by colony PCR and confirmed by Sanger sequencing. Verified strains were preserved as 15% glycerol stocks at −80 °C.

2.3. Validation of the biosynthetic modules

2.3.1. Production of hesperetin from naringenin

BL21-Hes harbouring pET28a-ThF3′H-CPR-MpOMT was grown overnight in LB medium containing kanamycin. The culture was inoculated at 1% (v/v) into 25 mL of fresh medium and grown at 37 °C and 180 rpm to an OD_{600} of approximately 0.6. IPTG and naringenin dissolved in DMSO were then added to final concentrations of 0.5 mM and 20 g/L, respectively. The temperature was reduced to 25 °C, and fermentation was continued for 24 h.

2.3.2. Production of neohesperidin from hesperetin

The downstream module was evaluated using BL21-Neohes harbouring pET28a-VvRHM-NRS-UGT73B2-Cm1,2RhaT. The strain was cultured and induced as described above. At 3 h after IPTG induction, hesperetin

dissolved in DMSO was added to a final concentration of 3 g/L. Fermentation was continued at 25 °C and 180 rpm for 48 h.

2.3.3. Complete-pathway production from naringenin

All six biosynthetic genes were assembled into pET28a(+) to generate BL21-Hes-Neohes, which contained the complete four-step pathway from naringenin to neohesperidin. Cells were grown at 37 °C to an OD_{600} of approximately 0.6. IPTG (0.5 mM) and naringenin (20 g/L) were then added, and fermentation was continued at 25 °C for 48 h. Samples were collected every 12 h to monitor hesperetin and neohesperidin production. BL21-Hes, BL21-Neohes and wild-type BL21 (DE3) were included as controls.

2.4. Acid-responsive neohesperidin biosynthesis

2.4.1. Characterization of the acid-responsive promoter

To evaluate the response of the P_cadBA promoter to acidic conditions, P_cadBA was placed upstream of the mRFP reporter gene, and the resulting reporter plasmid was transformed into E. coli DH5α. Reporter strains were cultured at pH 5.8 or 7.3 at 37 °C and 180 rpm. OD_{600} and mRFP fluorescence were measured every 4 h using excitation and emission wavelengths of 584 and 607 nm, respectively. Fluorescence intensity was normalized to OD_{600}.

2.4.2. Acid-responsive production of neohesperidin

PcadBA, whereas VvRHM-NRS and UGT73B2 remained IPTG-inducible. Engineered cells were grown to an OD_{600} of approximately 1.2 and transferred to M9 medium adjusted to pH 5.8 or 7.3. Hesperetin and IPTG were added to final concentrations of 3 g/L and 0.5 mM, respectively. Fermentation was continued for 48 h, with samples collected every 12 h for neohesperidin quantification.For pH-responsive biosynthesis, Cm1,2RhaT was placed under the control of

2.5. HPLC analysis

Fermentation broth (0.5 mL) was mixed with an equal volume of methanol, vortexed and centrifuged at 13,500 rpm for 5 min. The supernatant was filtered through a 0.22-μm membrane before HPLC analysis.

Hesperetin was analysed using an Agilent 1200 HPLC system equipped with a diode-array detector and a ZORBAX Eclipse Plus C18 column (250 × 4.6 mm, 5 μm). The column temperature was 30 °C, the flow rate was 1.0 mL/min, the injection volume was 10 μL and the detection wavelength was 280 nm. Mobile phases A and B were HPLC-grade acetonitrile and 0.5% (v/v) aqueous acetic acid, respectively. The gradient was: 0–12 min, 85–75% B; 12–17 min, 75% B; 17–20 min, 75–50% B; 20–30 min, 50–25% B; 30–35 min, 25–5% B; and 35–40 min, 5–85% B.

Neohesperidin was analysed using a C18 column at 35 °C, with a flow rate of 1.0 mL/min, an injection volume of 10 μL and detection at 290 nm. Mobile phase A was water containing 0.1% trifluoroacetic acid, and mobile phase B was methanol containing 0.1% trifluoroacetic acid. The gradient was: 0–0.1 min, 10% B; 0.1–10 min, 10–40% B; 10–20 min, 40–60% B; 20–22 min, 60–10% B; and 22–25 min, 10% B.

Products were identified by comparing their retention times and UV spectra with those of authentic standards and quantified using the external-standard method.

2.6. Statistical analysis

Data are presented as mean ± s.d. from at least three biological replicates. Comparisons between two groups were performed using Student's *t*-test, whereas multiple-group comparisons were conducted using one-way

analysis of variance followed by Tukey's post hoc test. $p < 0.05$ was considered statistically significant, and $p < 0.01$ was considered highly significant.

3. Results

3.1. Hesperetin-to-neohesperidin

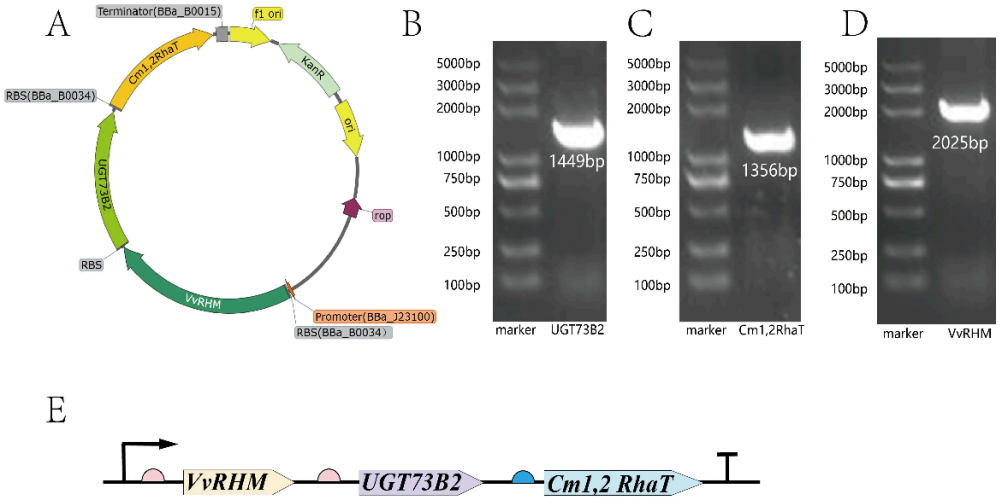

Figure 1. Construction of neohesperidin synthesis system. (A) Plasmid map of pET28a-VvRHM-UGT73B2-Cm1,2RhaT; (B–D) Agarose gel electrophoresis showing successful cloning of UGT73B2, Cm1,2RhaT, and VvRHM; (E) Gene circuit diagram of the neohesperidin biosynthetic pathway

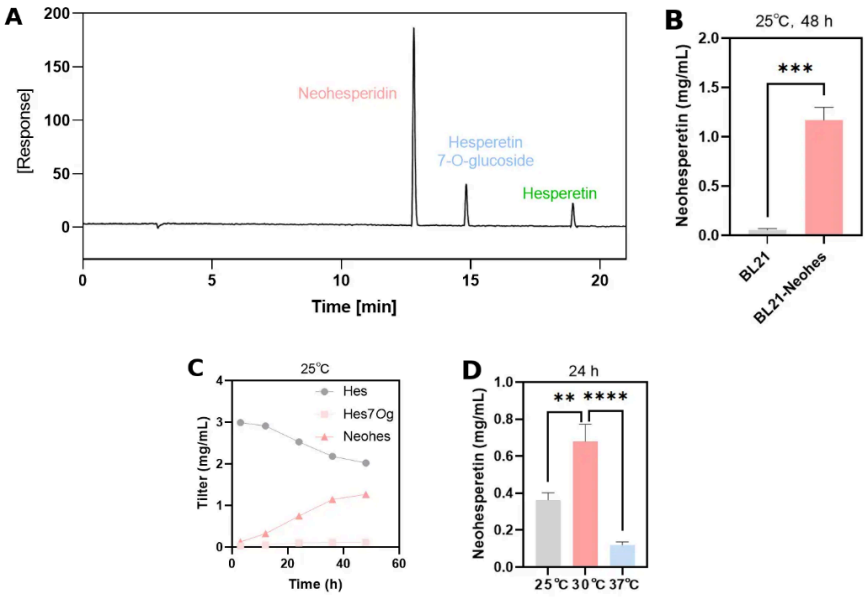

Figure 2. BL21-Neohes was induced with 0.5 mM IPTG and supplemented with 3 g/L hesperetin. (A) Representative HPLC chromatograms of the engineered and wild-type strains. (B) Neohesperidin titres after fermentation at 25 °C for 48 h. (C) Time course of neohesperidin production at 25 °C. (D) Effect of cultivation temperature on neohesperidin production, with the highest titre obtained at 30 °C

The downstream neohesperidin biosynthetic module was first constructed by coexpressing UGT73B2, VvRHM-NRS and Cm1, 2RhaT in Escherichia coli BL21 (DE3), generating the engineered strain BL21-Neohes. Restriction digestion and agarose gel electrophoresis produced DNA fragments of the expected sizes, confirming successful assembly of pET28a-VvRHM-NRS-UGT73B2-Cm1, 2RhaT (see Figure 1A–E).

Following supplementation with 3 g/L hesperetin, HPLC analysis of BL21-Neohes revealed a product peak corresponding to that of the authentic neohesperidin standard. No corresponding peak was detected in the wild-type control (see Figure 2A). After fermentation at 25 °C for 48 h, the neohesperidin titre of BL21-Neohes reached 1.17 ± 0.09 mg/mL, whereas the value measured in the wild-type control was 0.05 ± 0.01 mg/mL (see Figure 2B). Only trace amounts of hesperetin 7-O-glucoside were detected, consistent with its effective conversion during the terminal rhamnosylation step. Temperature screening showed that the highest neohesperidin production was obtained at 30 °C (see Figure 2C and D).

3.2. Acid responsive promoter

To evaluate the response of P_cadBA to acidic conditions, mRFP was placed under its control to generate the pSB1A3-P_cadBA-mRFP reporter construct. Successful assembly of the reporter system was confirmed by agarose gel electrophoresis (see Figure 3A–E).

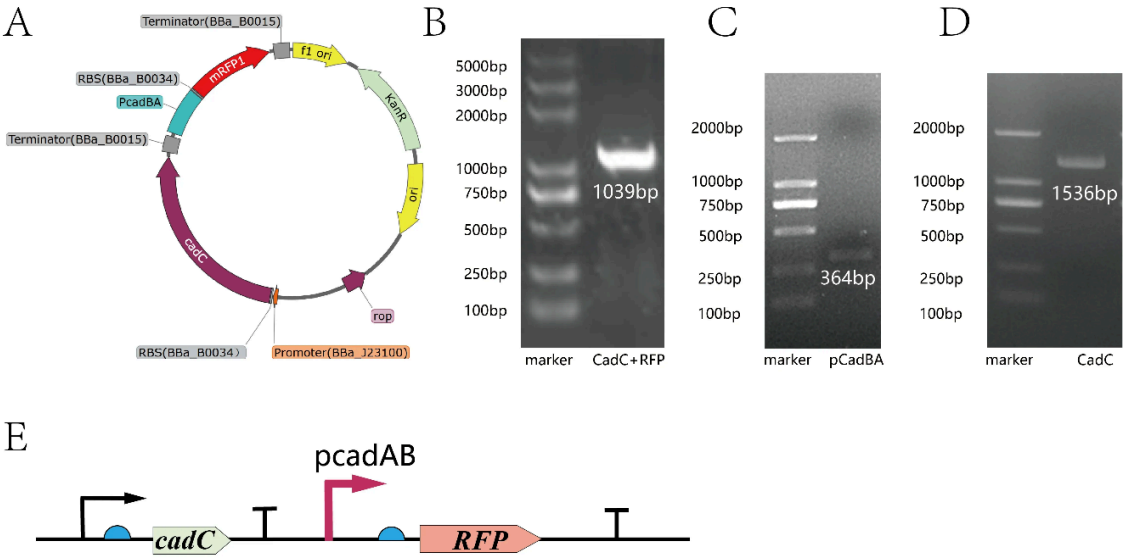

Figure 3. Acid-responsive biosensor construction. (A) Plasmid map of pSB1A3-P_cadBA-mRFP. (B–D) Agarose gel electrophoresis of the DNA fragments used to assemble the reporter construct. (E) Schematic representation of the P_cadBA-regulated mRFP reporter circuit

At pH 5.8, normalized mRFP fluorescence increased with cultivation time and rose markedly after approximately 12 h. The normalized fluorescence reached 265.31 ± 18.74 AU after 48 h. In contrast, fluorescence remained low at pH 7.3 and reached only 12.43 ± 3.21 AU at 48 h (see Figure 4A). This represented an approximately 21.3-fold increase at pH 5.8, and the difference between the two pH conditions was statistically significant ($p < 0.01$). The growth profiles under the two conditions were broadly similar, although low pH caused a modest reduction in cell growth (see Figure 4B). These results demonstrated that P_cadBA mediated strong acid-responsive expression with a limited effect on cell growth.

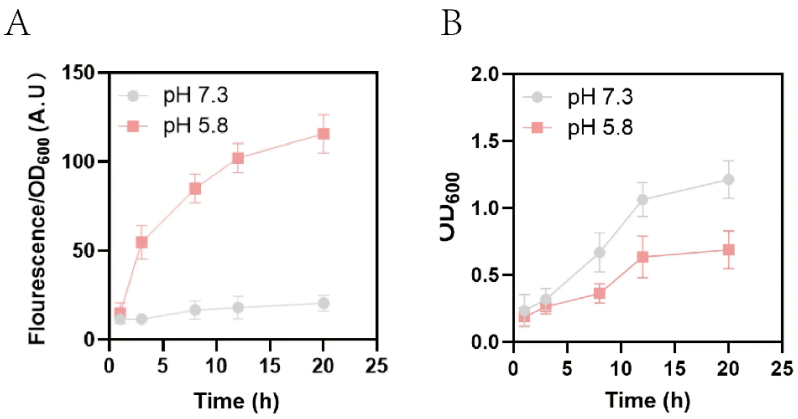

Figure 4. Functional characterization of the acid-responsive promoter pCadBA. (A) Normalized mRFP fluorescence over 48 h at pH 5.8 and 7.3. Acidic conditions resulted in an approximately 21.3-fold increase in fluorescence at 48 h. (B) OD_{600} profiles of the reporter strain under the two pH conditions

3.3. Neohesperidin in tumor microenvironment

Following validation of P_cadBA, Cm1,2RhaT, which encodes the enzyme responsible for terminal rhamnosylation, was placed under its control. In the resulting construct, VvRHM-NRS and UGT73B2 remained IPTG-inducible, whereas Cm1,2RhaT was regulated by extracellular pH. The insertion of P_cadBA and the associated regulatory fragments was confirmed by agarose gel electrophoresis (see Figure 5A–D).

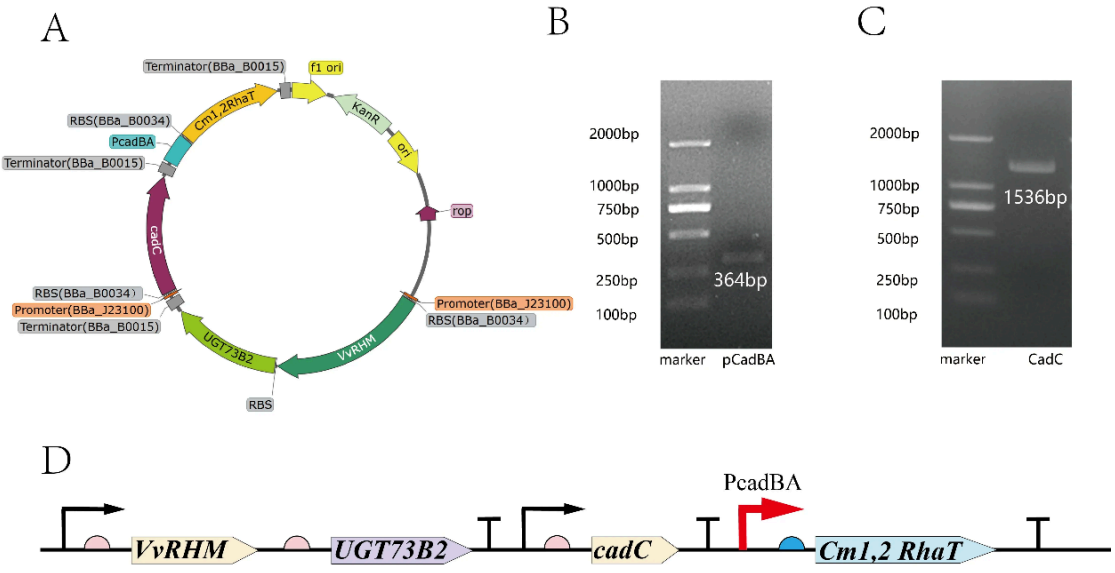

Figure 5. Neohesperidin synthesis system responsive to acid. (A) Plasmid map of VvRHM-NRS-UGT73B2-P_cadBA-Cm1,2RhaT. (B,C) Agarose gel electrophoresis confirming the insertion of P_cadBA and the associated regulatory fragment. (D) Schematic representation of pH-regulated Cm1,2RhaT expression controlling the terminal rhamnosylation step

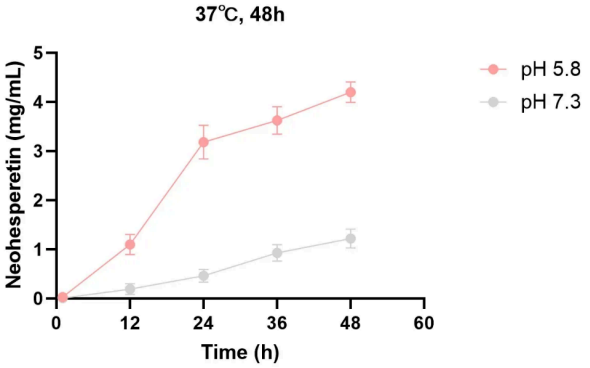

Figure 6. Neohesperidin accumulation was measured every 12 h during 48 h of fermentation at pH 5.8 and 7.3. The titre at pH 5.8 was 3.4-fold higher than that at pH 7.3 after 48 h ($P < 0.01$)

Neohesperidin production by the resulting strain was strongly dependent on culture pH. After 48 h, neohesperidin titres reached 4.20 ± 0.28 mg/mL at pH 5.8 and 1.22 ± 0.11 mg/mL at pH 7.3. The titre under acidic conditions was therefore 3.4-fold higher than that under neutral conditions, and the difference was statistically significant ($p < 0.01$). Time-course analysis further showed progressive neohesperidin accumulation at pH 5.8 (see Figure 6). These results demonstrated that P_cadBA-regulated terminal rhamnosylation increased neohesperidin production under acidic culture conditions.

3.4. Naringenin-to-hesperetin

An upstream biosynthetic module was constructed to produce hesperetin from naringenin and thereby eliminate the requirement for exogenous hesperetin. The module coexpressed ThF3′H, CPR and MpOMT in BL21(DE3), generating the engineered strain BL21-Hes. Agarose gel electrophoresis confirmed the successful insertion of all three genes into pET28a(+) (see Figure 7A–E).

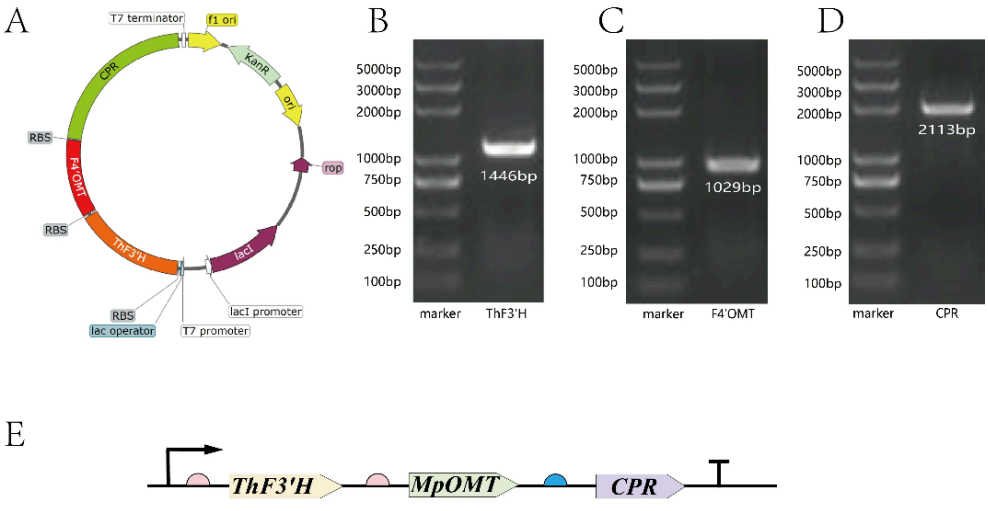

Figure 7. Construction of the synthesis system for hesperetin. (A) Plasmid map of pET28a-ThF3′H-CPR-MpOMT. (B–D) Agarose gel electrophoresis confirming the insertion of ThF3′H, CPR and MpOMT. (E) Schematic representation of the naringenin-to-hesperetin pathwayHPLC of the engineered strain (BL21-Hes) revealed a hesperetin peak that was not shown at all when doing the wild-type BL21 cultures

After supplementation with 20 g/L naringenin, HPLC analysis of BL21-Hes revealed a hesperetin peak that was absent from the wild-type BL21(DE3) control (see Figure 8A). After 24 h of fermentation, the hesperetin titre reached 11.91 ± 0.73 mg/mL, whereas the value measured in the wild-type control was 0.21 ± 0.04 mg/L (see Figure 8B). These results confirmed that the upstream module supported the conversion of naringenin to hesperetin.

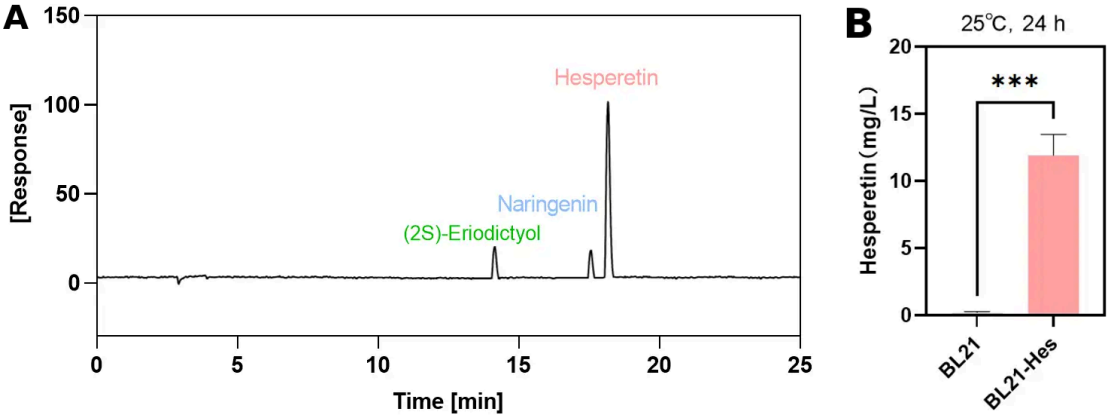

Figure 8. BL21-Hes was cultured with 20 g/L naringenin. (A) Representative HPLC chromatograms of BL21-Hes and wild-type BL21(DE3). The hesperetin peak was detected only in the engineered strain. (B) Comparison of hesperetin titres in the engineered and wild-type strains after 24 h of fermentation

3.5. Production of neohesperidin from naringenin

The upstream and downstream modules were subsequently combined to generate the complete-pathway strain BL21-Hes-Neohes. The six-gene construct contained ThF3′H, CPR, MpOMT, VvRHM-NRS, UGT73B2 and Cm1,2RhaT, enabling the conversion of naringenin to neohesperidin within a single host (see Figure 9A–E).

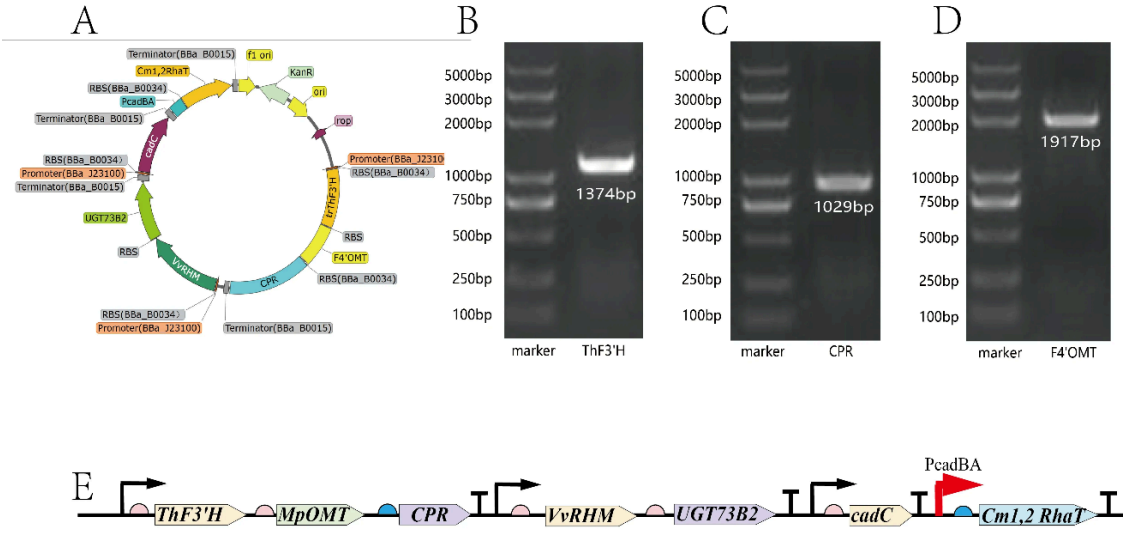

Figure 9. Synthesis system for hesperetin to neohesperidin. (A) Plasmid map of the six-gene construct. (B–D) Agarose gel electrophoresis confirming the insertion of the upstream pathway genes. (E) Schematic representation of the integrated naringenin-to-hesperetin-to-neohesperidin pathway

After fermentation with 20 g/L naringenin for 48 h, BL21-Hes-Neohes produced 4.55 mg/L neohesperidin, whereas the control produced 0.06 mg/L (see Figure 10). Neohesperidin production from naringenin demonstrated functional coupling of the hydroxylation, methylation, glucosylation and rhamnosylation reactions within the engineered host. Together, these results established a complete microbial pathway for converting naringenin into neohesperidin.

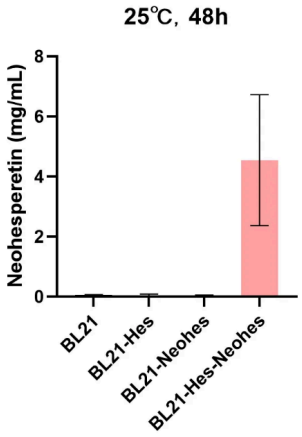

Figure 10. Neohesperidin titres were compared among wild-type BL21(DE3), the two single-module strains and the complete-pathway strain BL21-Hes-Neohes after IPTG induction and fermentation with 20 g/L naringenin at 25 °C for 48 h

4. Discussion

4.1. Rational design of a multi-functional probiotic therapeutic platform

This study describes the engineering and experimental testing of an integrated probiotic therapeutic system that aims to overcome three challenges in CRC treatment: delivering drugs at a desired location in space, scalability and consistency of production of bio-active natural flavonoids and the need for stringent safety controls of live biotherapeutic agents in clinical and environmental applications. Overall, the results show that synthetic biology has the potential to fill these gaps, by packing several functional programs into a single microbial chassis. However, Escherichia coli Nissle 1917, the typical probiotic chassis for intestinal delivery, was not itself engineered or validated in this study.

4.2. Biosynthetic pathway performance and metabolic flux considerations

The whole process of four generations' iterative optimization of the neohesperidin production pathway resulted in useful information on the metabolic constraints controlling the metabolic pathway of flavonoid glycoside biosynthesis in E. coli. The three-enzyme glycosylation cascade was introduced into BL21 (DE3) and supplemented with exogenous hesperetin (23-fold higher than the yield of the wild-type, without the cascade, with 1.17 mg/mL). A low amount of the intermediate hesperetin-7-O-glucoside meant there was little side product formation in the cascade, and that this cascade worked with high metabolic flux concentration, suggesting good enzyme co-expression. The temperature of the growth optimized the titres which were 1.42mg/mL at 30°C, as previously reported, heterologously expressed plant enzymes, such as cytochrome P450-class enzymes and glycosyltransferases are very temperature sensitive. The third generation hesperetin

synthesis module was able to produce 11.91 mg/mL of hesperetin from naringenin, partly thanks to the engineered mutant MpOMT S142V with a crucial amino acid change yielding an enzyme that is more selective for eriodictyol than for naringenin, which reportedly reduces non-productive methylation of naringenin by more than 90% [14]. Technical feasibility of both modules (4.55 mg/L of neohesperidin as the major product) was achieved in the fourth generation strain. The reduction in yield for the integrated system is probably due to competition for the substrates, the metabolic burden of expressing six heterologous genes at once and/or enzyme stoichiometry problems.

4.3. pH-responsive targeting and tumor microenvironment specificity

One of the most clinically important engineering accomplishments of this project is the acid responsive pCadC system [15]. The pH of the tumor microenvironment of CRC is around 5.8-6.5, which is attributed to the Warburg effect where aerobically glycolytic tumour cells release protons as well as lactate into the extra-cellular space. This acidity increases Matrix Metalloproteinases (MMPs) activity which aids the invasion of tissues, decreases the activity of cytotoxic immune cells and induces epithelial-mesenchymal transition [16-18]. The responsiveness cascade manifested itself as a 3.4-fold higher yield of neohesperidin in acidic conditions as opposed to neutral conditions when introduced into the neohesperidin synthesis pathway. Basal transcriptional leakage from pCadC (neutral condition) is still present and needs to be improved using different sequences for the transcriptional insulator or by adding other control mechanisms like riboswitches. Importantly, these pH gradients in the intestinal lumen are very dynamic depending on the composition of the diet, the intestinal motility and the fermentation by microbes. Before clinical translation, validation under physiologically-relevant conditions, which involve an environment close to the human intestinal one, will be crucial.

4.4. Comparison with alternative neohesperidin production strategies

The results obtained from this work are comparable to the shortcomings of the conventional phytochemical extraction method. The yields of neohesperidin from citrus fruit are less than 0.3% and the extraction process is a multi-step chromatographic purification step which is difficult to scale, dependent on the quality of raw material and the season and is incompatible with high purity pharmaceutical manufacturing requirements. The microbial fermentation method works under standard controlled conditions which can be standardized and monitored continuously and can be easily scaled-up using standard bioreactor infrastructure. Studies on microbial neohesperidin production in the past have been generally dependent on costly and expensive exogenous addition of flavonoids as expensive starting materials [19]. This work is an important step towards a full de novo synthesis that could be expanded upstream by introducing genes for the phenylpropanoid and flavonoid biosynthetic pathways that would allow naringenin to be synthesized from glucose as a single carbon source.

4.5. Limitations and future directions

There are a number of limitations. In order to achieve this, all the biosynthetic and biosafety experiments were performed in BL21 (DE3) or DH5α, and not in the desired therapeutic chassis EcN. In the case of differences in metabolic background, regulatory network architecture and codon usage between these strains, differences in expression levels and yields in EcN might be affected. It is therefore essential to validate all the constructs in EcN in a more intestinal-like environment. In vitro pH conditions used to validate the pCadC system are well matched to tumor microenvironment pH values reported in the literature, but fail to account for the multiple layers of the CRC intestinal milieu, immune cell infiltrates, different oxygen levels and other

microbial communities. The efficacy of in vitro targeting and drug release behavior will need to be validated in vivo in appropriate animal models of oral cancer or Azoxymethane (AOM) and Dextran Sulfate sodium (DSS) induced murine colitis-associated cancer to confirm that it is physiologically relevant. No direct measurement of the antitumor effectiveness of bacterially produced neohesperidin was made and the measured yield is total extracellular and intracellular concentration which may not correlate directly with bioavailability of the drug at the surface of the tumor cells. To demonstrate a functional connection between biosynthetic output and against tumor activity, future studies with cell viability assays using CRC cell lines (e.g., HCT116 or SW480) and conditioned media from engineered strains, or direct co-culture assays, will be required.

5. Conclusion

Finally, this research provides a well-defined synthetic biology pathway for the manufacture and specific delivery of neohesperidin through a live engineered E. coli to produce a live biotherapeutic agent. The results show that microbial biosynthesis can overcome yield and consistency issues of conventional extraction processes for neohesperidin, pH-responsive gene circuits can be used to create a highly environmentally discriminatory route to the production of drugs that are specifically targeted to tumors, and dual kill-switch systems can be used to achieve layered biosafety controls that are suitable for clinical use. This work provides a modular and extensible proof of concept for intelligent probiotic systems to be used as adjuvants in CRC therapy and sets the technical foundations for future in vivo validation and clinical translation studies.

References

[1] Hossain, M. S., Karuniawati, H., Jairoun, A. A., Urbi, Z., Ooi, D. J., John, A., Lim, Y. C., Kibria, K. M. K., Mohiuddin, A. K. M., Ming, L. C., Goh, K. W., & Hadi, M. A. (2022). Colorectal cancer: A review of carcinogenesis, global epidemiology, current challenges, risk factors, preventive and treatment strategies. *Cancers, 14*(7), 1732. https://doi.org/10.3390/cancers14071732

[2] International Agency for Research on Cancer. (n.d.). Cancer today. *World Health Organization*. Retrieved August 30, 2025, from https://gco.iarc.who.int/today/

[3] Sung, H., Siegel, R. L., Laversanne, M., Jiang, C., Morgan, E., Zahwe, M., Cao, Y., Bray, F., & Jemal, A. (2024). Colorectal cancer incidence trends in younger versus older adults: An analysis of population-based cancer registry data. *The Lancet Oncology, 26*, 51–63.

[4] Moshawih, S., Lim, A. F., Ardianto, C., Goh, K. W., Kifli, N., Goh, H. P., Jarrar, Q., & Ming, L. C. (2022). Target-based small molecule drug discovery for colorectal cancer: A review of molecular pathways and in silico studies. *Biomolecules, 12*(7), 878. https://doi.org/10.3390/biom12070878

[5] Suarez, J., Herrera, M. D., & Marhuenda, E. (1998). In vitro scavenger and antioxidant properties of hesperidin and neohesperidin dihydrochalcone. *Phytomedicine, 5*(6), 469–473.

[6] Wang, R., You, W., Lin, H., Cao, Y., Xu, C., Chen, K., Liu, Y., & Li, X. (2023). Naringin, neohesperidin and their corresponding dihydrochalcones as bioactive substances: A symphony of bitter–sweet. *Food Quality and Safety, 7*, Article fyad036. https://doi.org/10.1093/fqsafe/fyad036

[7] Sinha, D., Satapathy, T., Jain, P., Prasad, J., Sahu, D., Sahu, B., Verma, A., Singh, S., Verma, K., & Rathore, R. (2019). In vitro antidiabetic effect of neohesperidin. *Journal of Drug Delivery and Therapeutics, 9*, 102–109. https://doi.org/10.22270/jddt.v9i6.3633

[8] He, D., Gao, X., Wen, J., Zhang, Y., Yang, S., Sun, X., Cui, M., Li, Z., Fu, S., Liu, J., & Liu, D. (2024). Orally administered neohesperidin attenuates MPTP-induced neurodegeneration by inhibiting inflammatory responses and regulating intestinal flora in mice. *Food & Function, 15*(3), 1460–1475. https://doi.org/10.1039/d3fo04714h

[9] Wang, Y., Xie, R., Jia, S., Li, Y., & Qiao, Y. (2024). Research progress in the relationship between gut microbiota and Parkinson's disease. *Acta Microbiologica Sinica, 64*(10), 3610–3619.

[10] Cao, X., Li, L., Hu, J., Zhu, S., Song, S., Kong, S., Zhou, L., & Huang, Y. (2025). Neohesperidin protects against colitis-associated colorectal cancer in mice via suppression of the NF-κB/p65 and MAPK pathways. *The Journal of Nutritional Biochemistry, 136*, Article 109804. https://doi.org/10.1016/j.jnutbio.2024.109804

[11] Gong, Y., Dong, R., Gao, X., Li, J., Jiang, L., Zheng, J., Cui, S., Ying, M., Yang, B., Cao, J., & He, Q. (2019). Neohesperidin prevents colorectal tumorigenesis by altering the gut microbiota. *Pharmacological Research, 148*, Article 104460. https://doi.org/10.1016/j.phrs.2019.104460

[12] Akhter, S., Arman, M. S., Tayab, M. A., Islam, M. N., & Xiao, J. (2024). Recent advances in the biosynthesis, bioavailability, toxicology, pharmacology, and controlled release of citrus neohesperidin. *Critical Reviews in Food Science and Nutrition, 64*(15), 5073–5092.

[13] Yu, M., Hu, S., Tang, B., Yang, H., & Sun, D. (2023). Engineering Escherichia coli Nissle 1917 as a microbial chassis for therapeutic and industrial applications. *Biotechnology Advances, 67*, 108202.

[14] Liu, J., Xiao, Z., & Zhang, S. (2023). Restricting promiscuity of plant flavonoid 3′-hydroxylase and 4′-O-methyltransferase improves the biosynthesis of (2S)-hesperetin in E. coli. *Journal of Agricultural and Food Chemistry, 71*(25), 9826–9835.

[15] Küper, C., & Jung, K. (2005). CadC-mediated activation of the cadBA promoter in Escherichia coli. *Journal of Molecular Microbiology and Biotechnology, 10*(1), 26–39.

[16] Damgaci, S., Ibrahim-Hashim, A., Enriquez-Navas, P. M., Pilon-Thomas, S., Guvenis, A., & Gillies, R. J. (2018). Hypoxia and acidosis: Immune suppressors and therapeutic targets. *Immunology, 154*(3), 354–362. https://doi.org/10.1111/imm.12917

[17] Rankin, E. B., & Giaccia, A. J. (2016). Hypoxic control of metastasis. *Science, 352*(6282), 175–180.

[18] Corbet, C., & Feron, O. (2017). Tumour acidosis: From the passenger to the driver's seat. *Nature Reviews Cancer, 17*(10), 577–593.

[19] Koirala, N., Thuan, N. H., Ghimire, G. P., Van Thang, D., & Sohng, J. K. (2016). Methylation of flavonoids: Chemical structures, bioactivities, progress and perspectives for biotechnological production. *Enzyme and Microbial Technology, 86*, 103–116.